https://doi.org/10.2352/CIC.2025.33.1.5

Preferred skin color reproduction under mixed illumination

Liqing Wang[1], Ming Ronnier Luo[1], Yuechen Zhu[1]
[1] State Key Laboratory of Extreme Optical Instrumentation, Zhejiang University,China.

Abstract

Skin tone reproduction has long been a challenge in image processing due to illumination by multiple sources in real-world conditions. This paper describes an algorithm to achieve preferred skin tone reproduction. The work comprises two pivotal components including to develop: 1) a CCT-SPQ/D optimization model via controlled experiments to reveal the mapping relationships between correlated color temperature (CCT) and skin preference quality (SPQ) and chromatic adaptation degree (D), and 2) a novel white balance correction algorithm for skin regions under mixed illumination, which integrates local processing and spatial filtering with color temperature adaptive enhancement via the aforementioned model. Finally, a preference assessment experiment was conducted to demonstrate the superiority of the algorithm proposed.

1. Introduction and related work

Skin tone is one of the most critical and perceptually sensitive visual attributes in facial image processing, serving as a cornerstone for automatic face beautification algorithm.

Preferred reproducing skin color not only enhances the performance of downstream tasks but also substantially elevates user visual satisfaction. However, real-world lighting environments are often highly complex, typically involving multiple light sources with different spectral distributions and color temperatures. These mixed illumination conditions can lead to local inconsistencies, color temperature shifts, and color distortions of skin appearance.

Therefore, achieving preferred skin tone reproduction under mixed illumination conditions has become an important research topic in the fields of image processing.

Conventional automatic white balance (AWB) algorithms typically assume a single light source in the scene, which often fails to correct color casts effectively under mixed illumination conditions. Furthermore, human perception of skin tone is highly sensitive—any slight color deviation can be noticed, detracting the aesthetic appeal of the images.

In the research field of white balance, a lot of previous algorithms have been proposed, such as gray-world, white patch, edge based gray-world[1], gamut mapping[2], shade of gray[3], machine learning based white balance and so on[4-7]. These algorithms are all founded on the assumption of a single light source in the scene. Therefore they perform poorly when processing images captured under mixed illumination conditions.

Additionally, many white balance algorithms tailored for mixed illumination scenes have been proposed[8,9,10]. These approaches are mainly based on machine-learning or statistical method, and get quite promising results. However, memory colors, which are critical in image quality assessment and color constancy[11], are not considered. To address the importance of memory color, a preferred skin tone based image reconstruction algorithm for mixed illumination environments is proposed as a complementary solution. This method reconstructs the preferred appearance of skin tones under complex lighting conditions, thereby significantly enhancing the visual appeal of the resulting images.

2. Preferred skin reproduction under uniform illumination

In this section, a preference based skin tone white balance algorithm and experimental investigations of skin tone preferences across varying color temperature conditions will be introduced. The findings from these two components constitute essential elements of the later proposed preferred skin color reproduction algorithm for mixed illumination scenarios.

2.1 Memory color white balance

In previous research, a skin tone based illumination estimation algorithm has been proposed[12]. The detailed workflow of the algorithm is shown in Figure 1. This method is implemented mainly in two steps: first, extracting skin region pixels through face detection and skin segmentation and computing the mean CIE $L^*a^*b^*$ color center; second, estimating the light source based on the discrepancy between the image's skin tone center and the standard skin tone center from the Preferred Memory Color (PMC) Chart[13].

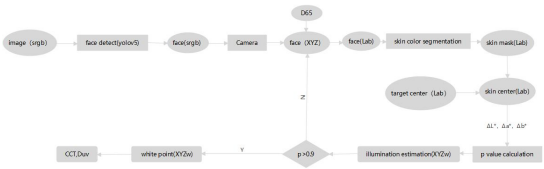

Figure 1 *Workflow of the previously proposed skin tone based illumination estimation method.*

This skin tone based illumination estimation algorithm substantially aids local white balance in mixed illumination scenarios, and provides essential support for the subsequent estimation of the CCT of each divided skin block.

2.2 Preferred skin rendering and adaptation experiment

Perceived skin appearance varies under light sources with differing CCTs. Consequently, determining optimal values for two perceptual rendering parameters—redering degree (skin preference quality, spq)[12] and the chromatic adaptation degree (D) under specific CCT condition becomes critical. To address this, experiments across a range of illumination color temperatures to determine the optimal preference based spq and D values for skin tones under varying lighting conditions.

The experimental procedure can be divided into three parts:

1. The image and data collection.
2. Preferred skin tone rendering and chromatic adaptation.
3. Subjective evaluation experiment.

2.2.1 The image capture and pre-processing

In this research, a datasets was prepared to investigate the relationship between preference rendering, chromatic adaptation degree and CCT.

A standardized illumination environment was established for this study, encompassing a color temperature range from 3000 K to 9000 K, with detailed spectral data recorded for each individual light source. During data acquisition, models, uniformly attired in

black outerwear, were seated within the standardized lighting environment. A standard PMC Chart[13] was positioned on the chest of each model. Image capture was performed using the OPPO Find X6pro smartphone. The shooting parameters were configured as follows: aperture f/1.8, shutter speed 1/100 s, ISO sensitivity 320, and white balance locked at 6500 K. A RAW format image were acquired for each capture.

The standardized preprocessing pipeline was implemented as follows[14,15]: original RAW images in DNG format were decoded into TIFF format using dcraw software. Then the TIFF format images underwent demosaicing to reconstruct full-color RGB data. Then the Auto White Balance (AWB) gain matrix and Color Correction Matrix (CCM) were computed based on the measured Spectral Sensitivity Function (SSF)[16] of the OPPO X6 Pro smartphone and the recorded spectral data of actual light sources. Demosaiced images were sequentially processed by AWB correction and CCM mapping. At last, linear RGB data was transformed to the sRGB color space through γ -correction to generate the result.

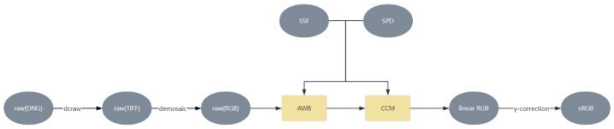

Figure 2. *Workflow of raw image processing.*

2.2.2 Preferred skin tone rendering and chromatic adaptation

Upon completion of the aforementioned RAW preprocessing pipeline, sRGB images referenced to the D65 standard white point were obtained; subsequent skin tone preference rendering within the D65 white space was then employed to enhance subjective appeal, followed by a Chromatic Adaptation Transform (CAT16[17]) to achieve a harmonious fusion of the rendered skin tone and the original atmosphere of the scene.

The first part is the preference skin tone rendering. Basing on the preferred skin tone centers defined in the PMC Chart, preference based rendering can be applied to enhance the visual appeal of the skin tones.

Preference rendering is accomplished by shifting the mean CIE L*a*b* value of the skin tone region toward the preferred memory color center for the corresponding category in the PMC Chart. During the rendering process, the parameter spq is utilized to control the degree of the preference adjustment[18-22].

The calculation formula for spq is listed below. Specific parameter values can be found in the relevant PMC Chart publications[12,13].

$$spq = \frac{1}{1+e^{\Delta E-\alpha}} \quad (1)$$

$$\Delta E = \sqrt{\begin{matrix} k_1 * (L - L_s)^2 + k_2 * (a - a_s)^2 + \\ k_3 * (b - b_s)^2 + k_4 * (a - a_s) * (b - b_s) \end{matrix}} \quad (2)$$

Equation 1 and 2 are skin color ellipse equation in PMC Chart.

k_1-k_4, α, are ellipse parameters. L_s, a_s, b_s are prefer memory skin color ellipse center. When spq=0.5, the equation represents a 50% preference skin ellipsoid in CIELAB color space.

The second part is the chromatic adaptation. Following skin tone enhancement taking D65 as the white point for preference improvement, chromatic adaptation transformation (CAT16 model[17]) is applied with the input white point configured as D65 and the output white point set to the recorded real scene illumination parameters. By modulating the degree of adaptation factor D, this process achieves optimized visual harmonization between skin tones and environmental illumination while partially preserving the chromatic characteristics of the original lighting environment.

All images obtained from the acquisition and pre-processing stages underwent systematic skin preference rendering and chromatic adaptation processing. With the spq parameter ranging from 0.5 to 1.0 in 0.1 increments and the degree of chromatic adaptation (D) ranging from 0 to 1.0 in 0.2 increments, each RAW image was processed through 6×5 parameter combinations to yield 30 distinct rendered images.

2.2.3 Subjective evaluation experiment

The experiment employed two Chinese adult models (one male, one female), and seven uniform light source differed in CCT ranging from 3000K to 9000K were used. For each CCT, 30 parametrically rendered images were generated. The subjective evaluation comprised 231 valid assessment units (7 CCTs × 30 images × (1+10% repeats)) utilizing a 6-point preference scale (-3 to +3), where negative scores indicate dislike, positive scores denote like, and absolute values correlate directly with preference intensity.

During the subjective evaluation, models were seated under spectral consistent illumination conditions replicating the original capture setup. Images rendered from corresponding color temperature sessions were displayed on mobile devices characterized by GOG (Gain-Offset-Gamma) model calibration[23]. Observers were instructed to evaluate preference scores based on comparative assessment between processed images and the live appearance of skin tones under actual scene illumination. The experiment followed a block-wise progression: rendered images were presented in color temperature groups. Upon completion of all ratings within a given temperature group, both displayed content and ambient lighting were synchronously switched to the next target color temperature. A mandatory 30-second visual adaptation period was enforced post-transition before initiating subsequent evaluations. This procedure iterated until all seven color temperature groups were assessed.

In Figure 3 below, shows the environment of subjective evaluation experiment.

Figure 3. *The setup for the skin preference subjective evaluation experiment.*

2.2.4 Experiment result

The experiment involved 26 observers divided by model gender. Inter-observer variability analysis revealed maximum stress-inter values of 52.63% (Mean = 35.01%) for female model evaluations, and 47.48% (Mean = 34.42%) for male model evaluations. Given high cross-gender consistency (group difference <1%), the aggregated global stress-inter reached 52.63% (M = 35.08%). Intra-observer stability assessment demonstrated a mean stress-intra of 9.57% across all participants,

indicating excellent rater self-consistency. Collectively, these metrics confirm the statistical reliability of experimental data.

For each rendered image, the preference factor P was calculated as the percentage of observers assigning positive ratings (indicating preference). These (spq, D, P) triplets were categorized by capture color temperature and visualized as 3D surface distribution plots shown in Figure 4 below.

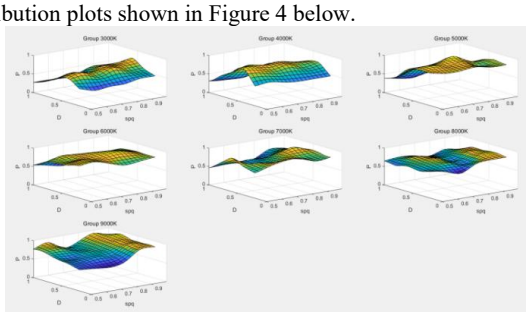

Figure 4. *(spq ,D, P) 3D surface distribution plots*

It can be seen from the distribution map above in Figure 4, in low CCT range (3000K-5000K), chromatic adaptation degree (D) dominates preference (P) with negligible spq impact. And the D value maximizing P increases monotonically with CCT. And in high CCT range (>5000K), the impact of D is significantly reduced , while spq emerges as the primary determinant, and the spq value yielding peak P exhibits positive correlation with CCT.

This result is consistent with expectations. Under low color temperature conditions, the perceived skin color differences are reduced compared to the actual differences, thereby diminishing the influence of skin color rendering while amplifying the role of chromatic adaptation. As the color temperature increases, the impact of chromatic adaptation on skin appearance weakens, whereas the effect of skin color rendering becomes more pronounced, ultimately emerging as the dominant factor.

To elucidate the inter-dependencies among spq, D, and P across CCT and identify optimal parameter ranges, a granular analysis was performed. For each CCT, all data points(N=400 per CCT) were sorted in descending order of P value, with the top 20% highest rated samples (n=80 per CCT) extracted. These elite samples were projected onto spq-P and D-P planes respectively to characterize functional relationships, as is shown in Figure 5 below.

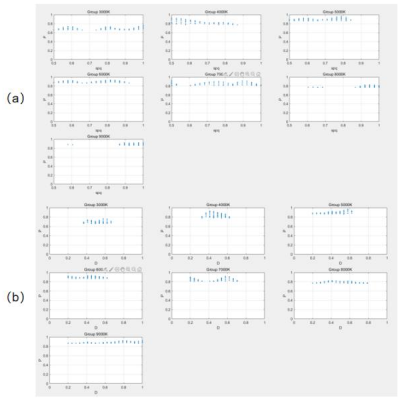

Figure 5. *Top 20% points projected onto P-spq and P-D planes.*

In Figure 5, (a) represents the P-spq plane. At lower CCT(3000K-5000K), P shows negligible correlation with SPQ, with high P points dispersed across spq ∈ [0.5,1.0]. Increasing CCT shifts the distribution centroid toward higher spq. Above 8000K, high-P samples concentrate at spq close to1.0. While (b) represents P-D plane. For lower CCT, high P values correspond to mainly D ∈ [0.4,0.6] , indicating an optimal D range. Scatter data with higher CCT, confirming the effect of D diminished.

To elucidate the inter-dependence between CCT-spq and CCT-D relationships, high-preference samples were projected onto CCT-spq and CCT-D planes respectively. Parametric fitting was applied to derive functional dependencies.

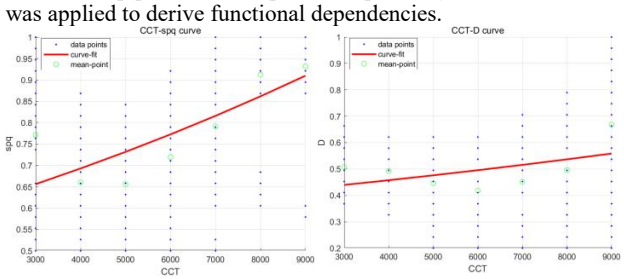

Figure 6. *High preference points and the curve fitted between CCT-spq and CCT-D.*

As is shown in Figure 6, functional curves were fitted through mapping high-P samples on CCT-spq and CCT-D planes.

The equations are listed below:

$$spq = 0.5571 * e^{\frac{0.0545*CCT}{1000}} \quad (1)$$

$$D = 0.3899 * e^{\frac{0.0399*CCT}{1000}} \quad (2)$$

Correlation between fitted curves and experimental data was rigorously evaluated by computing the arithmetic mean of data points per CCT, thereby quantifying model prediction accuracy. The fitted curves exhibit correlation coefficients (r_1=0.8010(CCT-spq), r_2=0.4935(CCT-D)), attributable to parametric dominance shifts, at low CCT (<5000K), spq minimally impacts P with D being the dominant factor, optimal D selection enables high P across arbitrary spq within valid ranges. Conversely, high CCT (>8000K) show diminished D influence with spq dominance, where optimized spq ensures robustness to D variation. Crucially, implementing CCT-spq/D selection via fitted curves consistently achieves high preference scores, validating the model's efficacy.

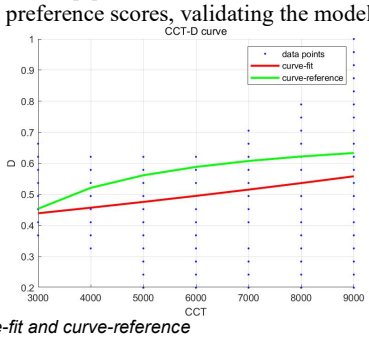

Figure 7. *Curve-fit and curve-reference*

Then, further incorporated reference CCT-D curves from prior literature for comparative validation was reported. As is shown in Figure 7, the red curve represents our fitted result while the green curve depicts the CCT-D reference model in previous research[24]. The curves demonstrate exceptional consistency across the full CCT spectrum (3000K-9000K) with a correlation coefficient of r=0.9512, and both reside within the high-preference zone, providing double-blind verification of the parametric model's scientific validity.

3. Preferred skin reproduction under mixed illumination

The workflow of the algorithm proposed in this research can be seen in Figure 8. The algorithm consists of three main stages. First, skin regions are detected and extracted to focus subsequent processing on facial areas. Second, the image undergoes local white balance based on a previously proposed memory color white balance algorithm[12], and then the CAT16 model[17] is used to map the results to the D65 space. Third, within the D65 space, skin tones are reconstructed according to the PMC Chart and then the CAT16 model is used again to convert the image back to its original color-temperature space. Then after the skin region's segmentation and replacement, getting the output result.

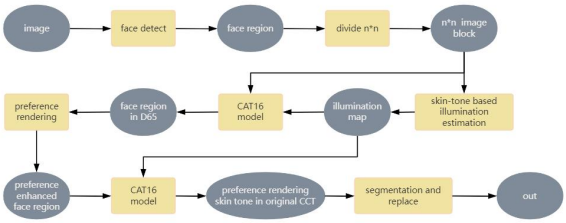

Figure 8. *workflow of preferred skin color reproduction under mix illumination.*

3.1 Datasets

To facilitate skin tone preference reconstruction under mixed illumination conditions, a dedicated datasets was collected. In the laboratory, a dual light source system with adjustable color temperature and luminance was installed, symmetrically positioned on either side of a centrally seated model. By varying the color temperatures of the two sources, the model's facial skin was illuminated under different color temperature conditions on the left and right sides. Frontal images were then captured to form a skin tone datasets under mixed illumination.

The photographed subjects include four ethnic groups, Chinese, South Asians, Caucasians, and Africans, with both male and female models represented. The adjustable light sources cover a color-temperature range from 3000K to 9000K. 10 mixed illumination types are included in the datasets, as is listed in Table 1 below. During capture, all models wore black clothing and carried a standard PMC Chart on their chest.

Table 1. Mixed illumination type.

number	1	2	3	4	5
left	A	A	D38	D38	D38
right	4000K	6000K	5000K	6000K	7600K
number	6	7	8	9	10
left	5000K	5000K	5000K	7500K	7500K
right	3000K	4000K	6000K	3000k	4000K

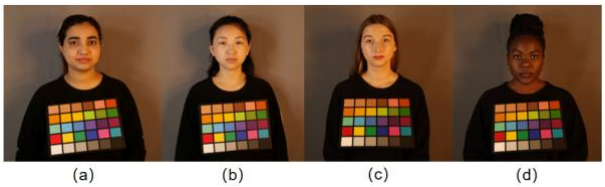

Figure 9. *An example of images in datasets.*

From a to d in Figure 9, the images depict South Asian, Chinese, Caucasian, and African female models, respectively, photographed under certain standard mixed illumination conditions.

3.2 Local white balance

Building upon the aforementioned algorithm, this work further introduces a local white balance approach to skin regions, wherein illumination estimation is independently performed for each sub-block to generate a spatially varying illumination distribution map.

The detailed process of local white balance is shown in Figure 10 below. (a) is the original image. The capture illumination is 5000K on the left and 3000K on the right. Upon inputting the original image, face detection is performed to localize the facial region (b). The facial region is then divided into n × n equal - sized blocks (c). For each block, a skin based illumination estimation algorithm is applied to obtain local illumination parameters, and the resulting estimates across all blocks are smoothed via spatial Gaussian filtering to produce a continuous distribution map (d). Then, the CAT16 model is employed for each block to transform from the estimated illumination to D65, and get the face region image in D65 (e). Then based on preferred skin color center in PMC Chart, the preference rendering is applied, get the result(f). At last, the CAT16 model and illumination map are used again to transfer the image back to its original illumination, get the output facial region(g).

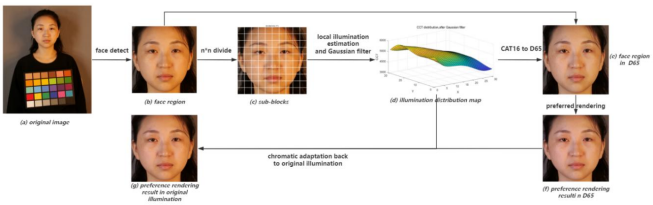

Figure 10. *Workflow of local white balance , preferred rendering and chromatic adaptation.*

3.3 Parameters experiment

In the above local white balance workflow, images are first divided into n×n blocks, with each block undergoing skin tone based illumination estimation, followed by spatial Gaussian filtering, and then transformation to the D65 illumination space via the CAT16 model.

In Figure 11, an example of the impact of parameters n and σ on the performance of the local white balance algorithm was shown. The first row illustrates the white balance results as the block size parameter n varies under the condition σ=1. The second row illustrates the white balance results as the Gaussian filter standard deviation σ varies under the condition n=20. The last col image(e) is the corresponding image capture under D65, used as the ground truth to evaluate the performance of the algorithm.

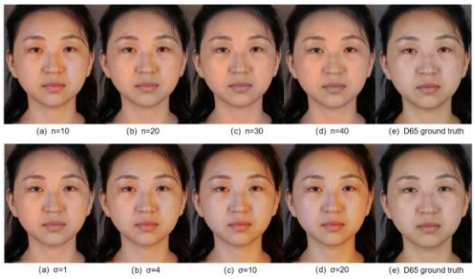

Figure 11. *An example of the impact of parameters n and σ on the performance of the local white balance algorithm.*

It's obvious from the result shown in Figure 11 that the selection of block number n and filter standard deviation σ is

critical to the outcome. So, in order to identify the optimal parameters set, a series of experiments were conducted: processing the same image set with varying n and σ values, using images captured under a standard D65 illumination in the laboratory as ground truth, and computing the color differences of skin tone pixels between processed images and the ground truth to evaluate the performance of the local white balance method.

The block size parameter n was varied from 10 to 50 in increments of 10, yielding five levels, while the Gaussian filter standard deviation σ was set to eight values: 0.5, 1, 2, 4, 6, 10, 15, 20. The surface plot illustrating the relationship between the color difference and the parameters n and σ were shown in Figure 12. From (a) to (d) correspond to the results for South Asians, Chinese, Caucasians, and Africans, respectively. The plotted data represent the mean color differences computed from all subjects of each ethnicity across all images captured under mixed illumination conditions.

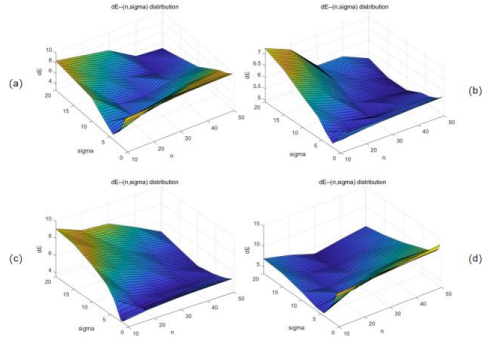

Figure 12. *The figure presents a surface distribution plot illustrating the impact of parameters n and σ on the color difference.*

As is shown in Figure 12, for the parameter combinations (n,σ) that minimize the color difference, a near-linear relationship is observed between the two. This finding aligns with theoretical expectations. Under the condition of a fixed skin region area, increasing the block number n results in smaller block sizes and a greater number of blocks; conversely, a smaller n yields larger blocks and fewer subdivisions. Spatial Gaussian filtering is employed to smooth the estimated values between adjacent blocks. Taking the smoothing effect on the forehead and facial skin as an example, as n increases, the number of blocks spanning the forehead and face also increases; to maintain a similar smoothing weight across different n values, a larger σ should be selected accordingly. Consequently, the figure demonstrates that when n and σ vary linearly, the color difference remains approximately constant.

Table 2 below presents the optimal σ values and the minimum corresponding color differences for each ethnic group when n=30.

Table 2. Minimum color differences and σ for each ethnic group when n=30.

ethnic	Caucasian	Chinese	South Asian	African
n	30	30	30	30
σ	5	5	10	15
DE	3.73	5.0	3.70	3.67

3.4 Skin preference rendering and chromatic adaptation

Following the determination of optimal local AWB parameters through prior parametric studies, skin regions under mixed illumination were mapped to the D65 space.

Subsequent application of skin preference enhancement and chromatic adaptation transformation aimed to reverse the image back to the original color temperature space, achieve simultaneous enhancement of skin tone appeal and preserve chromatic harmony with environmental illumination.

In order to achieve this, in this phase the CCT-spq (Correlated Color Temperature - Skin Preference Quality) and CCT-D (CCT - Adaptation Degree) mapping models derived from prior experiments in this research were tried to integrated into the local optimization framework. Leveraging the color temperature distribution map generated during local AWB, each sub-block is dynamically assigned SPQ and D parameters corresponding to its specific CCT, enabling temperature aware adaptive enhancement.

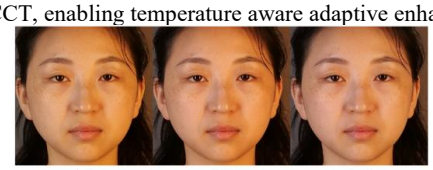

Figure 13. *An example of skin tone preference reconstruction under mixed illumination.*

Figure 13 shows an example of skin tone preference reconstruction under mixed illumination. In Figure 13, (a) represents the original skin tone region under mixed illumination. After applying local white balance and preference based rendering, if the spq and D are uniformly set to 1 when transforming back to the original mixed illumination environment, the resulting image is shown in (b). By employing the relationship curve CCT-D and CCT-spq, the optimal spq, D value can be selected for each image block based on its CCT, yielding the final result in (c).

Visual comparisons demonstrate that processed image (b) enhances skin preference while partially preserving original illumination information compared to baseline (a), yet exhibits noticeable skin boundary in illumination transition areas. In contrast, the optimized result (c) integrates the proposed color temperature adaptive framework to achieve comparable preference enhancement with significantly improved skin tone gradation — manifesting smooth spectral transitions — while maintaining superior environmental lighting fidelity, thereby establishing enhanced chromatic coherence between skin and scene illumination.

3.5 Verification experiment

A preference evaluation experiment was conducted as follows: For each original mixed illumination image, a processed versions were generated — an adaptive parameter set (local dynamic assignment of spq/D values). These were paired with the original to form pairwise comparison. Observers were asked to evaluate them in terms of preference evaluation to quantify the efficacy of the processing strategies in enhancing skin region appeal under mixed illumination.

Figure 14. *The experiment GUI.*

A total of 17 participants were recruited to perform pairwise preference evaluations. The experimental datasets consisted of 80 image pairs, covering four ethnic groups, two genders, and 10 mixed-illumination combinations. In addition, 40 duplicate pairs were included to assess response consistency. Consequently, each participant completed 120 subjective evaluations in total.

The results indicate that images processed by the proposed algorithm achieved an average selection rate of 75.2%, whereas the original images were selected only 24.8% of the time. Furthermore, the preference selection results for each ethnic group are presented as follows: South Asian, 75.7%, Caucasian 72.9%, Chinese 73.8%, and African 78.5%.

The subjective evaluation results indicate that the proposed algorithm yields good improvements. Compared to the original images captured under mixed illumination conditions, the algorithm processed images exhibit increase in visual preference.

4. Conclusion

In this study, a skin tone enhancement algorithm framework was established. Step 1 is to transform the RAW images captured to the reference sRGB space with D65 illumination. Step 2 is to perform skin preference enhancement and chromatic adaptation experiment to derive CCT-spq and CCT-D mapping models for environmental adaptive optimization. Step 3 is to extend the previously proposed skin tone based white balance algorithm to mixed illumination scenarios through image zoning and spatial domain Gaussian filtering. Step 4 is to integrate local white balance followed by illumination specific preference rendering and chromatic adaptation to achieve skin tone adaptive enhancement under mixed illumination. This not only boost subjective preference while partially preserving original spectral characteristics. Finally, a preference verification experiment was conducted to demonstrate the superiority of the algorithm proposed here.

However, there are some limitations in the algorithm. One is that it is only considering Chinese skin colors. More skin colour types should be investigated in the future studies. Second is that only skin region is studied. Future research should include more memory colour. In addition, deep learning (CNN/Transformer architectures) with large scale mixed illumination datasets should be produced to achieve universal white balance algorithm, cascaded with this skin enhancement for holistic quality improvement.

5. References

[1] J. Van de Weijer, T. Gevers, and A. Gijsenij, "Edge-based color constancy," Ieee Transactions on Image Processing, vol. 16, pp. 2207-2214, Sep 2007.

[2] D. A. Forsyth, "A NOVEL ALGORITHM FOR COLOR CONSTANCY," International Journal of Computer Vision, vol. 5, pp. 5-36, Aug 1990.

[3] Finlayson, Graham D., and Eveline Trezzi. "Shades of Gray and Colour Constancy." Proceedings of the 12th Color Imaging Conference, 2001, pp. 37-41.

[3] J. T. Barron, Y. T. Tsai, and Ieee, "Fast Fourier Color Constancy," in 30th IEEE/CVF Conference on Computer Vision and Pattern Recognition (CVPR), Honolulu, HI, 2017, pp. 6950-6958.

[4] Y. M. Hu, B. Y. Wang, S. Lin, and Ieee, "FC4: Fully Convolutional Color Constancy with Confidence-weighted Pooling," in 30th IEEE/CVF Conference on Computer Vision and Pattern Recognition (CVPR), Honolulu, HI, 2017, pp. 330-339.

[5] M. Afifi, M. S. Brown, and Ieee, "Deep White-Balance Editing," in IEEE/CVF Conference on Computer Vision and Pattern Recognition (CVPR), Electr Network, 2020, pp. 1394-1403.

[6] M. Afifi, B. Price, S. Cohen, and M. S. Brown, "When Color Constancy Goes Wrong: Correcting Improperly White-Balanced Images," in 2019 IEEE/CVF Conference on Computer Vision and Pattern Recognition (CVPR), 2020.

[7] S. Bianco and R. Schettini, "Adaptive Color Constancy Using Faces," IEEE Trans Pattern Anal Mach Intell, vol. 36, pp. 1505-18, Aug 2014.

[8] Hui, Zhuo , et al. "Learning to Separate Multiple Illuminants in a Single Image." IEEE (2019).

[9] Afifi, Mahmoud , M. A. Brubaker , and M. S. Brown . "Auto White-Balance Correction for Mixed-Illuminant Scenes." (2021).

[10] David Serrano-Lozano, Aditya Arora , and M.S. Brown, et al. "Revisiting Image Fusion for Multi-Illuminant White-Balance Correction." Computer Vision and Pattern Recognition(CVPR), 2025.

[11] J. J. M. Granzier and K. R. Gegenfurtner, "Effects of memory colour on colour constancy for unknown coloured objects," I-Perception, vol. 3, pp. 190-215, 2012.

[12] Liqing Wang, Yuechen Zhu, Xiaoxuan Liu, Ming Ronnier Luo, "Improve Image White Balance by Facial Skin Color" in Color and Imaging Conference, 2023, pp 43 - 48

[13] M. R. Luo, “The New Preferred Memory Color (PMC) Chart,” Color Research and Application 49, no. 6 (2024): 564–576, https://doi.org/10.1002/col.22940.

[14] Ramanath, Rajeev , et al. "Color image processing pipeline." IEEE Signal Processing Magazine 22.1(2005):34-43.

[15] Rowlands, D. Andrew . "Color conversion matrices in digital cameras: a tutorial." Optical Engineering 59.11(2020).

[16] Hui Fan, Ming Ronnier Luo, "Comparison of LED-based and reflective colour targets for camera spectral sensitivities estimation" in Color and Imaging Conference, 2022.

[17] C. J. Li, Z. Q. Li, Z. F. Wang, Y. Xu, M. R. Luo, G. H. Cui, et al., "Comprehensive color solutions: CAM16, CAT16, and CAM16-UCS," Color Research and Application, vol. 42, pp. 703-718, Dec 2017.

[18] H. Z. Zeng and R. Luo, "Preferred Skin Color Enhancement for Photographic Color Reproduction," in Conference on Color Imaging XVI - Displaying, Processing, Hardcopy, and Applications, San Francisco, CA, 2011.

[19] H. Z. Zeng, R. Luo, and Is, "Preferred Skin Colours of Africans, Caucasians, and Orientals," in 19th Color and Imaging Conference - Color Science and Engineering Systems, Technologies, and Applications, San Jose, CA, 2011, pp. 211-216.

[20] R. Peng, M. R. Luo, Y. C. Zhu, X. X. Liu, and M. Pointer, "Preferred skin reproduction of different skin groups," Vision Research, vol. 207, p. 15, Jun 2023.

[21] M. K. Cao and M. R. Luo, "Preferred skin tones on mobile displays under illuminants having different correlated colour temperatures," Vision Research, vol. 198, p. 12, Sep 2022.

[22] M. K. Cao, M. R. Luo, Y. Lu, and K. Xaio, "A study of preferred and natural memory colours across different ethnic groups," Color Research and Application, vol. 48, pp. 178-200, Mar 2023.

[23] A, Kaida Xiao , et al. "Visual gamma correction for LCD displays." Displays 32. 1(2011):17-23.

[24] Zhai, Qiyan , and M. R. Luo . "Study of chromatic adaptation via neutral white matches on different viewing media." Optics Express 26.6(2018):7724.